

NJC

Accepted Manuscript



This is an *Accepted Manuscript*, which has been through the Royal Society of Chemistry peer review process and has been accepted for publication.

Accepted Manuscripts are published online shortly after acceptance, before technical editing, formatting and proof reading. Using this free service, authors can make their results available to the community, in citable form, before we publish the edited article. We will replace this *Accepted Manuscript* with the edited and formatted *Advance Article* as soon as it is available.

You can find more information about *Accepted Manuscripts* in the [Information for Authors](#).

Please note that technical editing may introduce minor changes to the text and/or graphics, which may alter content. The journal's standard [Terms & Conditions](#) and the [Ethical guidelines](#) still apply. In no event shall the Royal Society of Chemistry be held responsible for any errors or omissions in this *Accepted Manuscript* or any consequences arising from the use of any information it contains.

A novel 8-hydroxyquinoline—pyrazole based highly sensitive and selective Al(III) sensor in purely aqueous medium with intracellular application: experimental and computational studies†

Abu Saleh Musha Islam^a, Rahul Bhowmick^a, Hasan Mohammad^a, Atul Katarkar^b, Keya Chaudhuri^b and Mahammad Ali^{a*}

(LINE INCLUDED FOR SPACING ONLY - DO NOT DELETE THIS TEXT)

A new 8-hydroxyquinolin-pyrazole based highly sensitive and selective Al³⁺ sensor, 8Q-NH-Pyz (H₂L³) was found to exhibit a turn-on fluorescence enhancement (FE) as high as 157 fold with K_d (1.76 ± 0.06) × 10⁻⁵ M. The 1:1 binding stoichiometry was revealed from the linear fit of (F_{max}-F₀)/(F-F₀) vs. 1/[Al³⁺] of the fluorescence titration data which was further substantiated by Job's method and HRMS studies. LOD determined by 3σ methods was found to be 4.29 nM and quantum yields determined to be 0.002 and 0.28 for the ligand and its Al³⁺ complex, respectively. The tentative coordination environment in the [Al(L³)(H₂O)]⁺ complex was delineated by DFT calculations. The TDDFT calculations reveal the spectral features comparable to the experimental ones. This constitutes the first report on the fluorescent sensing of Al³⁺ and hence F⁻ in purely aqueous medium.

Introduction

Molecular sensors are highly valuable tools for selective recognition of chemical and biological species.¹ Though, analyte selective molecular sensors are plenty in the literature the detection of Al³⁺ has always been a problematic task due to the lack of its spectroscopic characteristics and poor coordination ability.² Despite of being a non-essential element, the detection of Al³⁺ is of great interest due to its potential toxicity arising out of its widespread application in automobiles, computers, packaging materials, electrical equipment, machinery food additives and building construction.^{3,4} It is well known that 40% of soil acidity is due to aluminium toxicity.⁵

Although quite a number of analytical methods like chromatography⁶, accelerator mass spectroscopy (AMS)⁷, graphite furnace atomic absorption spectrometry (GFAAS)⁸, neutron activation analysis (NAA)⁹, inductively coupled plasma-atomic emission spectrometry (ICP-AES)¹⁰, inductively coupled plasma-mass spectrometry (ICP-MS)¹¹, laser ablation microprobe mass analysis (LAMMA)¹², electro thermal atomic absorption spectrometry (ETAAS)¹³ etc. are available, the fluorescence chemo sensing is found to be the best choice; as it is the simplest, sensitive, fast and inexpensive technique¹⁴ offering significant advantages over other methods.¹⁵ Hence, recently the design and synthesis of Al³⁺ selective fluorescent probes has received intense attention of the chemists.¹⁶⁻¹⁸ Compared to other metal ions, only a few fluorescent chemo sensors have been reported for the detection of Al³⁺.¹⁹⁻²⁵ For practical applications, it is necessary to develop Al³⁺ sensors that are easily prepared and possess selective and sensitive signalling mechanisms.

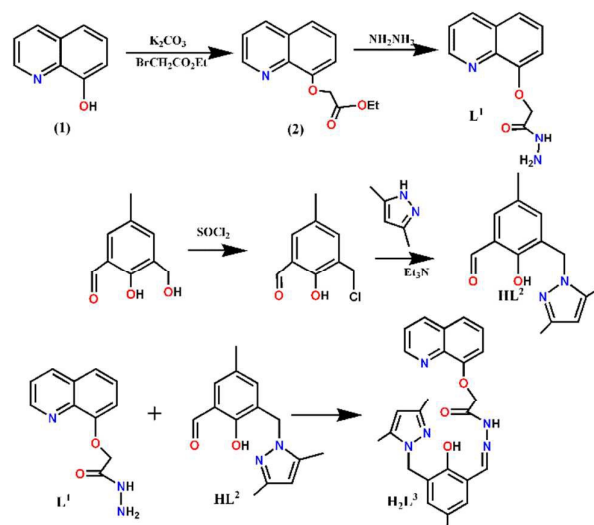
^aDepartment of Chemistry, Jadavpur University, 188, Raja Subodh Chandra Mullick Rd, Kolkata, West Bengal 700032, E-mail: m_ali2062@yahoo.com

^bDepartment of Molecular & Human Genetics Division, CSIR-Indian Institute of Chemical Biology, 4 Raja S.C. Mallick Road, Kolkata-700032, India.

† Electronic supplementary information (ESI) available: Detailed experimental procedures and additional spectroscopic data.

see DOI:*****

Here, we are reporting a highly selective Al³⁺ probe containing potential N₃O₃ donor atoms that binds selectively to Al³⁺ in presence of other metal ions. Although few reports on Al³⁺ ion sensors are available in the literature most of them are operative in non-aqueous or mixed aqueous solvents, but not in pure aqueous medium, except one, which was carried out at pH 7.4 in *tris* buffer (Table S1). Towards this end, we are going to disclose, for the first time, an Al³⁺ sensor (H₂L³) which operates in purely aqueous medium.



Scheme 1. Synthesis of targeted probe H₂L³.

Results and Discussion

(Quinolin-8-yloxy)-acetic acid ethyl ester, Quinolin-8-yloxy)-acetic acid hydrazide(L¹) and (3-(3,5-Dimethyl-pyrazol-1-ylmethyl)-2-hydroxy-5-methyl-benzaldehyde (HL²) were

synthesized as outlined in **Scheme 1**. The probe (8Q-NH-Pyz, H_2L^3) was then prepared by a simple Schiff base condensation between L^1 and HL^2 in MeOH. This ligand is suitable for Al^{3+} recognition and characterized by NMR (**Fig. S1, S2, S3, S4**), ESI-MS⁺ (**Fig.S5**) and IR studies (**Fig. S6**).

The UV-Vis spectrum of sensor **8Q-NH-Pyz** was recorded in 10 mM HEPES buffer at pH 7.2, which displayed well-defined bands at 330 nm. On gradual addition of Al^{3+} there is a decrease in absorbance at 330 nm along with the development of a new band at 380 nm (**Fig. 1**). This indicates a complexation between **8Q-NH-Pyz** and Al^{3+} . However, no such significant change in the absorption spectrum of **8Q-NH-Pyz** was observed with other tested metal cations.

In the absence of Al^{3+} , **8Q-NH-Pyz** is very weakly fluorescent owing to the combined effects of excited state intramolecular proton transfer (ESIPT) from phenolic -OH to azomethain-N and rotation across the C=N bond (cis/trans isomerization). The fluorescence enhancement observed for compound **8Q-NH-Pyz** in the presence of Al^{3+} ions was attributed to the chelation enhanced fluorescence (CHEF) effects arising through coordination of pyrazole-N, phoxido-O and amido-O, ethereal-O, quinoline-N along with one water molecule; as delineated by HRMS analysis and DFT calculations (vide infra). As a result of metal coordination both ESIPT and rotational isomerisation are efficiently blocked.

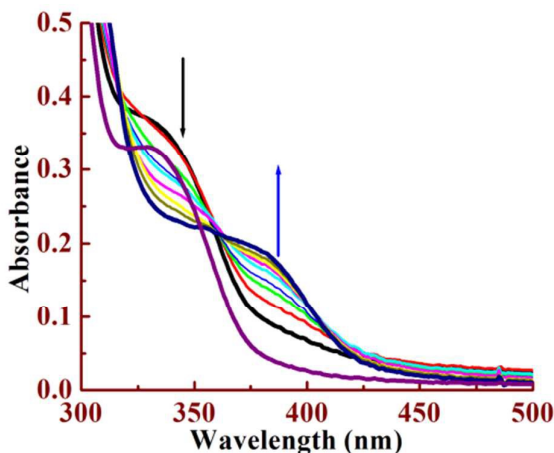


Fig. 1. Absorption titration of **8Q-NH-Pyz** (20 μ M) with Al^{3+} (0-200 μ M) in pH 7.2, 10 mM HEPES buffer.

The emission spectra of **8Q-NH-Pyz** and its fluorescence titration with Al^{3+} were recorded in 10 mM HEPES buffer at pH 7.2 (**Fig. 2**). A plot of F.I. vs. $[Al^{3+}]$ gives a non-linear curve with decreasing slope at higher concentration of Al^{3+} (**Fig S7**). A Benesi-Hilderband plot (**Eqn 1**) of $[F_{max}-F_0]/(F-F_0)$ vs. $1/[Al^{3+}]$ gives straight line with slope $K_d = (1.76 \pm 0.06) \times 10^{-5}$ M with complexation. The LOD of Al^{3+} calculated by using 3σ method was found to be 4.29 nM. (**Fig. S8**)

$$\frac{F_{max} - F_0}{F - F_0} = 1 + \frac{1}{[Al^{3+}]}$$
 Eqn 1

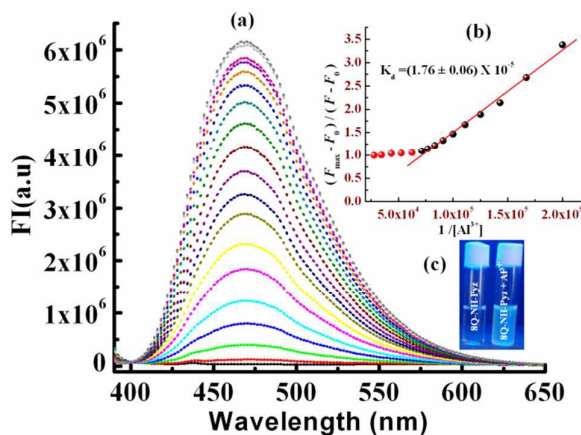


Fig.2 (a) Fluorescence titration of **8Q-NH-Pyz** (20 μ M) in pH 7.2, HEPES buffer by the gradual addition Al^{3+} with $\lambda_{ex} = 380$ nm, $\lambda_{em} = 470$ nm. Inset; (b) Benesi-Hilderbandplot; (c) UV exposed image.

A K_d value of $(1.76 \pm 0.06) \times 10^{-5}$ M unambiguously demonstrates a moderately strong binding of **8Q-NH-Pyz** towards Al^{3+} . The 1:1 stoichiometry of Al^{3+} complex with **8Q-NH-Pyz** was delineated by Job's Method (**Fig. S9**) was further confirmed by ESI-MS⁺ (m/z) mass spectrometry $[Al(8Q-NH-Pyz)(H_2O)]^+$ ($m/z = 485.65$) (**Fig. 3 & S10**) while that for $[8Q-NH-Pyz + H]^+$ is 444.2029. Al^{3+} detection was not perturbed by biologically abundant Na^+ , K^+ , Ca^{2+} etc. metal ions and several transition metal ions, namely Cr^{3+} , Mn^{2+} , Fe^{2+} , Fe^{3+} , Co^{2+} , Ni^{2+} , Cu^{2+} , and heavy metal ions like Cd^{2+} , Pb^{2+} (**Fig. 4**). Several anions also cause no interference (**Fig. 5**) except F^- .

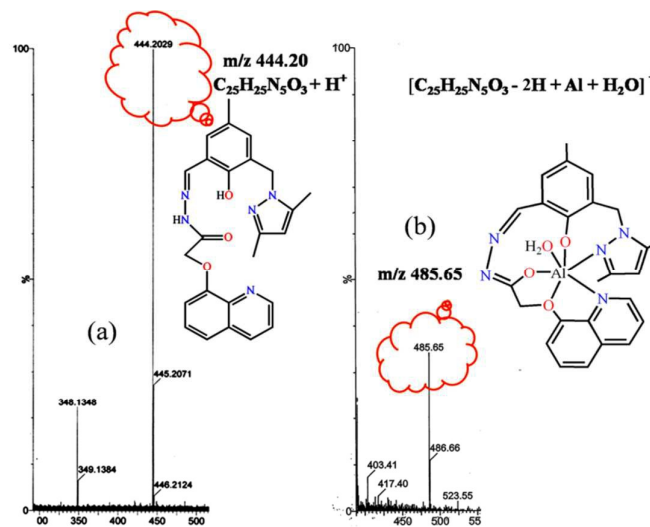


Fig.3. HRMS spectra of (a) **8Q-NH-Pyz** and (b) Al^{3+} -**8Q-NH-Pyz** complex in the positive mode.

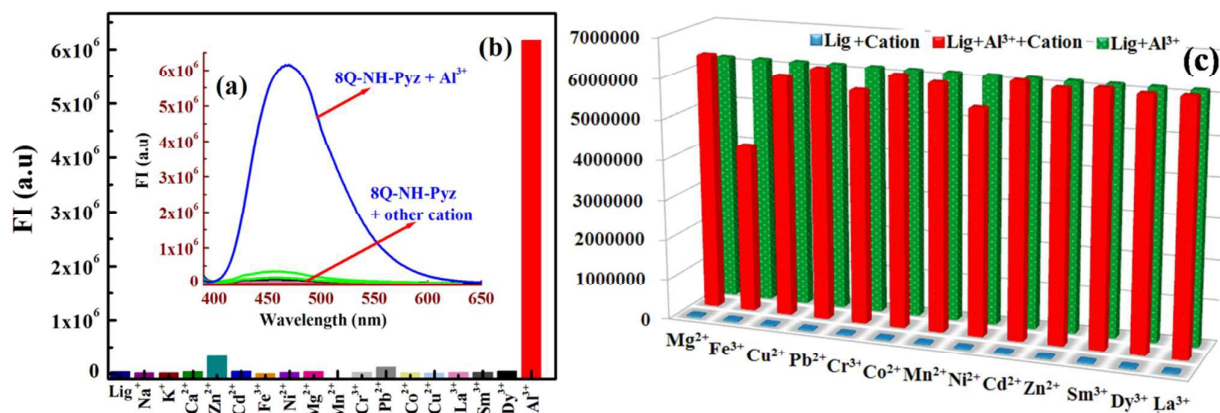


Fig. 4(a). Spectral plot of different cations; (b) Bar chart illustrating fluorescence response of **8Q-NH-Pyz** at 470 nm ($\lambda_{\text{ex}} = 380$ nm) towards different cations in HEPES buffer pH 7.2. Conditions: **8Q-NH-Pyz** = 20 μM , $\text{M}^{\text{n}+} = 80$ μM ; where, $\text{M}^{\text{n}+} = \text{Al}^{3+}$, Ca^{2+} , Cd^{2+} , Co^{2+} , Cr^{3+} , Cu^{2+} , Fe^{3+} , K^+ , Mg^{2+} , Mn^{2+} , Na^+ , Pb^{2+} , Zn^{2+} , Sm^{3+} , Dy^{3+} , La^{3+} . (c) Bar chart illustrating selectivity of Al^{3+} -**8Q-NH-Pyz** complex over other cations.

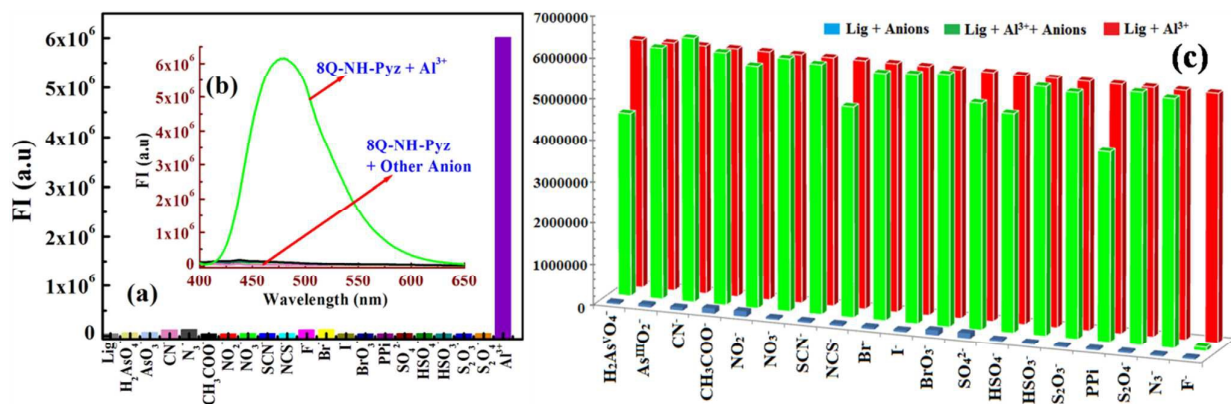


Fig.5. (a) Bar chart illustrating fluorescence response of **8Q-NH-Pyz** at 470 nm ($\lambda_{\text{ex}} = 380$ nm) towards different anions in HEPES buffer pH 7.2; (b) Spectral plot **8Q-NH-Pyz** in presence of different anions and Al^{3+} . **8Q-NH-Pyz** = 20 μM , $\text{X}^{\text{n}-} = 80$ μM ; where, anions are Cl^- , Br^- , I^- , F^- , SCN^- , NCS^- , CN^- , PPI^- , NO_3^- , NO_2^- , SO_4^{2-} , BrO_3^- , N_3^- , CH_3COO^- , $\text{S}_2\text{O}_3^{2-}$, $\text{S}_2\text{O}_4^{2-}$, HSO_4^- , HSO_3^- , AsO_4^{3-} , H_2AsO_4^- ; (c) Bar chart illustrating selectivity of Al^{3+} -**8Q-NH-Pyz** complex towards F^- ion in presence of other anions.

In order to support the binding of Al^{3+} with the receptor **8Q-NH-Pyz** the ^1H NMR titration was performed in $\text{DMSO}-d_6$ and D_2O (**Fig. 6 and Table 1**). The ^1H NMR spectrum of **8Q-NH-Pyz** contains signals for the $\text{HC}=\text{N}$ (azomethine, H) (f) at 8.46 ppm and phenolic -OH proton (b) at 11.74(s). The imine proton (a), quinoline protons (g) and (h) appear at 12.35(s), 8.96 (d) and 8.38(d) ppm, respectively. The other quinoline protons appear in the region 7.28-7.62 ppm. The chemical shifts for other protons appear in the usual positions. Addition of 1 equivalent of $\text{Al}(\text{NO}_3)_3 \cdot 9\text{H}_2\text{O}$ leads to a slight down field shift of azomethine proton (8.46 to 8.49 ppm) while phenolic -OH and imine protons vanish completely. All these clearly suggest the enol form $[\text{C}(\text{=N})(\text{OH})]$ of $\text{C}(\text{=O})\text{NH}$ group which on coordination to Al^{3+} losses the proton along with phenolic-OH. The quinoline protons (g) and (h) are down field shifted to 9.04 and 8.70 ppm respectively which again supports its participation to bonding

with Al^{3+} ion through quinolin-N atom. The other quinoline protons are also slightly down-field shifted.

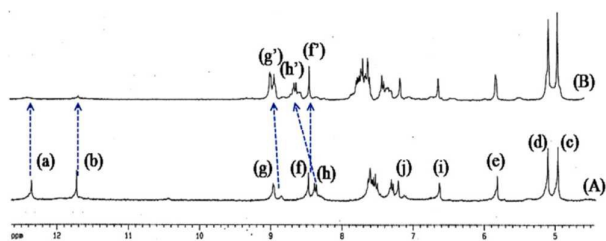


Fig.6. Selected portion of ^1H -NMR spectra of (A) **8Q-NH-Pyz** and (B) Al^{3+} -**8Q-NH-Pyz** complex.

Table 1. Selected chemical shifts of 8Q-NH-Pyz and Al^{3+} -8Q-NH-Pyz complex.

Proton No.	8Q-NH-Pyz (ppm)	8Q-NH-Pyz + Al^{3+} (ppm)
(a)	12.35	-
(b)	11.72	-
(f)	8.46	8.49
(g)	8.96	9.04
(h)	8.38	8.70

F⁻ Quenching. The advancement in fluorescent techniques make it possible to simultaneously monitor fluoride ions, in particular, sense and visualize it inside the living cells.²⁶ In order to study the reversible binding of Al^{3+} to 8Q-NH-Pyz a fluorescence quenching experiment was performed by titrating to 8Q-NH-Pyz- Al^{3+} complex prepared in situ by reacting 20 μM 8Q-NH-Pyz and 20 μM Al^{3+} against $[\text{F}^-]$ (0-20 μM) (Fig 7(a)). A plot of FI vs. $[\text{F}^-]$ gives a non-linear curve (Fig 7(b)).

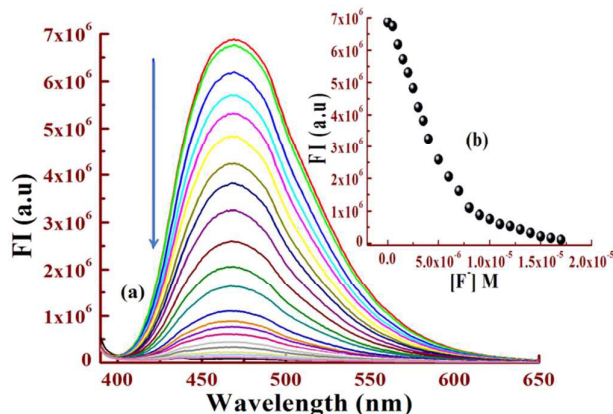


Fig. 7 (a) Fluorescence titration spectra of (8Q-NH-Pyz + Al^{3+} complex, 20 μM each) with TBAF (0-20 μM) in HEPES buffer pH 7.2. $\lambda_{\text{ex}} = 380 \text{ nm}$. **(b)** Plot of F.I. vs. $[\text{F}^-]$.

The reversibility of a probe is one of the essential requirements for sensing applications. Therefore, the reversibility of 8Q-NH-Pyz was examined by the alternate addition of Al^{3+} and F^- . As shown in Fig. 8, on the addition of Al^{3+} to a solution of 8Q-NH-Pyz a remarkable enhancement in emission intensity at 470 nm was observed. Again, on adding one equivalent of F^- , it effectively de-metallates Al^{3+} ion from 8Q-NH-Pyz- Al^{3+} complex leading to the bleaching of emission band at 470 nm. However, on further addition of Al^{3+} in slight excess of one equivalent to the resulting solution 8Q-NH-Pyz recovers its fluorescence up to 90% of its original value. This clearly establishes the reversible binding of Al^{3+} towards 8Q-NH-Pyz which is important for the fabrication of devices to sense the Al^{3+} .

pH-titration.

To study the practical applicability of the probe the effect of pH on the fluorescence response of 8Q-NH-Pyz towards Al^{3+} was

investigated. Experimental results showed that the free 8Q-NH-Pyz (10 μM) is very weakly fluorescent in the pH range 2.0-10. However, in presence of 18 μM of Al^{3+} the FI increases steadily with the increase in pH reaches a maximum at pH ~ 8.0 then decreases rapidly with further increase in pH (Fig.9). This observation clearly indicates the presence of different Al^{3+} species ($[\text{Al}(\text{H}_2\text{O})_5(\text{OH})]^{2+}$, $[\text{Al}(\text{H}_2\text{O})_2(\text{OH})_2]^+$, $[\text{Al}(\text{H}_2\text{O})_3(\text{OH})_3]$ and $[\text{Al}(\text{H}_2\text{O})_2(\text{OH})_4]^-$) and relative amounts changes with the change in pH. At pH ≥ 8.0 $[\text{Al}(\text{H}_2\text{O})_3(\text{OH})_3]$ species dominates and Al^{3+} comes out of the complex in this form and as a consequence FI decreases.

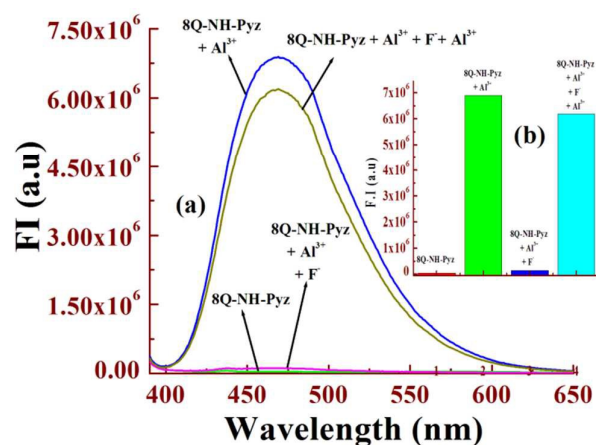


Figure 8. (a) Change in Fluorescence Intensity of 8Q-NH-Pyz (20 μM) upon addition of one equivalent of Al^{3+} and then 1 equivalent of F^- and regeneration of fluorescence upon further addition slight excess Al^{3+} . (b) is the corresponding bar plot. Conditions: HEPES buffer (10 mM) in water at pH 7.2., $\lambda_{\text{ex}} = 380 \text{ nm}$.

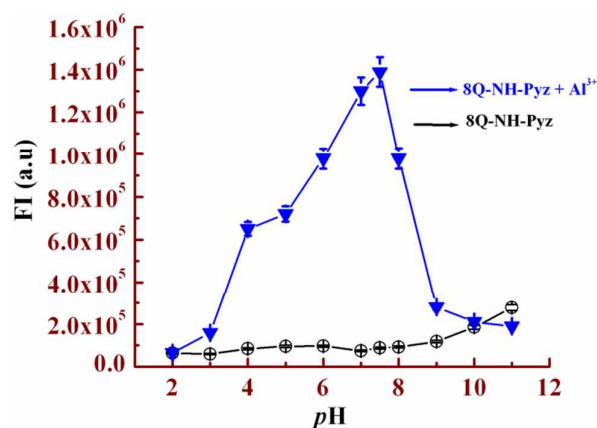


Fig. 9. Fluorescence intensity vs. pH plot at 470 nm 8Q-NH-Pyz 10 μM , (detonated by black circles) and 8Q-NH-Pyz + Al^{3+} complex (denoted in blue triangle).

Geometry optimization and electronic structure

The optimized geometry of 8Q-NH-Pyz (H_2L^3) and its Al^{3+} complex, $[\text{Al}(\text{L}^3)(\text{H}_2\text{O})]^+$, is shown in Fig. 10. Both H_2L^3 and $[\text{Al}(\text{L}^3)(\text{H}_2\text{O})]^+$ complex has $C1$ point group. The nature of all

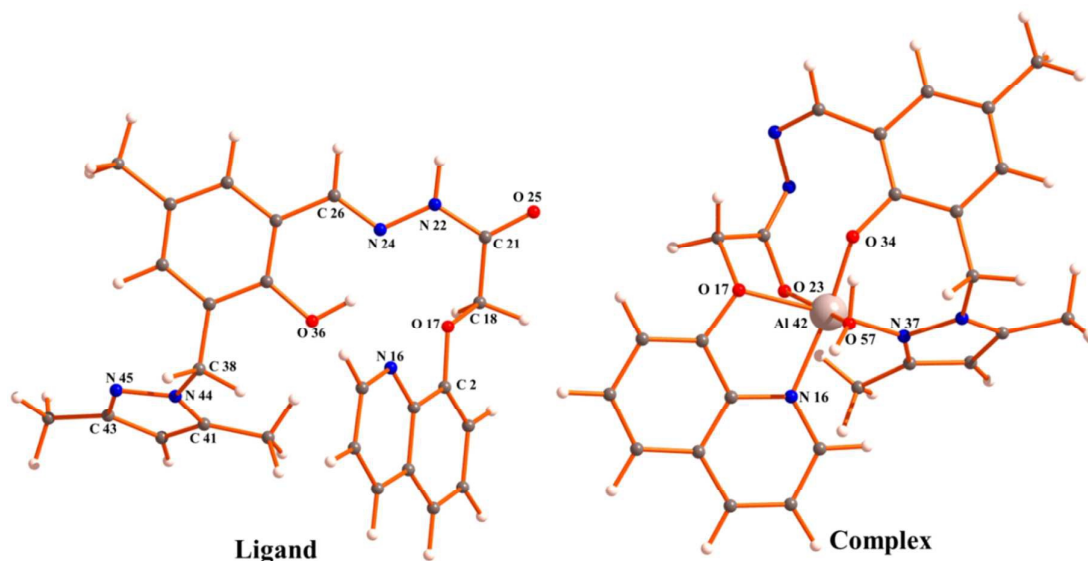


Fig. 10. Optimized geometry of ligand 8Q-NH-Pyz and complex $[Al(L^3)(H_2O)]^+$.

stationary points for both the free ligand and its Al^{3+} complex were confirmed by carrying out normal mode analysis. All the frequencies turned out to be positive, which proved the global minima of H_2L^3 and $[Al(L^3)(H_2O)]^+$. The composition of the complex as $[Al(L^3)(H_2O)]^+$ is based on HRMS studies which displayed the presence of one water molecules in the molecular fragment. The central metal is in octahedral geometry coordinated through pyrazole-N16, phenoxido-O34, amido-O23, ethereal-O17, quinoline-N37 along with one water molecule (O57). The geometry around the central metal atom is distorted octahedral, the basal plane being occupied by pyrazole-N16, quinoline-N37, pheoxido-O34 and ethereal-O17 while the axial positions are occupied by amido-O23 and water-O57.

It is important to note that the azomethane-N did not coordinate to metal center while the quinoline-N and ethereal-O coordinate to the metal centre probably to relive some steric strain imposed by the bulky 8-hydroxyquinoline moiety and methyl groups present in 3,5-dimethyl pyrazole rings. Some important optimized geometrical parameters of the free ligand and complex are listed in **Table S2** and **Table S3**.

In case of **8Q-NH-Pyz** in the ground state, the electron density resides mainly on HOMO-2, HOMO-3, HOMO-4 and LUMO+4 molecular orbitals of the pyrazole moiety as well as 2-hydroxy-5-methyl-benzaldehyde fragment of the ligand; while for HOMO and LUMO molecular orbitals a considerable contribution comes only from 2-hydroxy-5-methyl-benzaldehyde moiety. Again, in case of HOMO-1 and LUMO+1 molecular orbitals the electronic contributions come from the quinoline moiety. The energy gap between HOMO and LUMO is 4.09 eV (**Fig. 11**). In case of $[Al(L^3)(H_2O)]^+$ complex HOMO-2 and HOMO-1 molecular orbitals carries most of the electron density in the 2-hydroxy-5-methyl-benzaldehyde moiety while in LUMO orbital electron resides mainly on quinoline moiety

with HOMO – LUMO energy gap of 2.524 eV. These compositions are useful in understanding the nature of transition as well as the absorption spectra of both the ligand and complex.

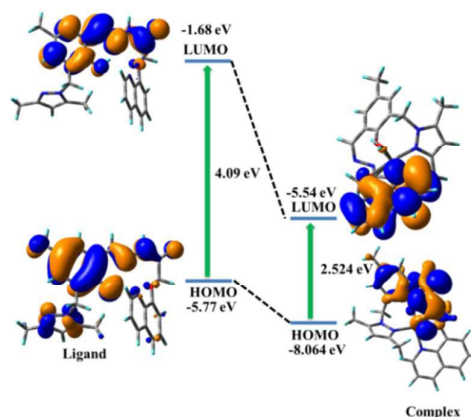


Fig. 11. Frontier molecular orbital of ligand **8Q-NH-Pyz** (H_2L^3) and complex $[Al(L^3)(H_2O)]^+$.

The ligand **8Q-NH-Pyz** shows three absorption bands at 336, 300, and 288 nm in aqueous medium at room temperature. These three bands are assigned to $S_0 \rightarrow S_1$, $S_0 \rightarrow S_4$ and $S_0 \rightarrow S_8$ electronic transitions, respectively (**Fig. S11**). The absorption energies along with their oscillator strengths are given in **Table S4**. The complex $[Al(L^3)(H_2O)]^+$ shows two absorption bands at 385 and 337 nm (**Fig. S12**) in water at room temperature and the corresponding calculated absorption bands are located at 382.26, and 335.16 nm which are in excellent agreement with our experimental results (**Table S5**). These two absorption bands can be assigned to the $S_0 \rightarrow S_2$, and $S_0 \rightarrow S_3$ transitions, respectively (**Table S5**).

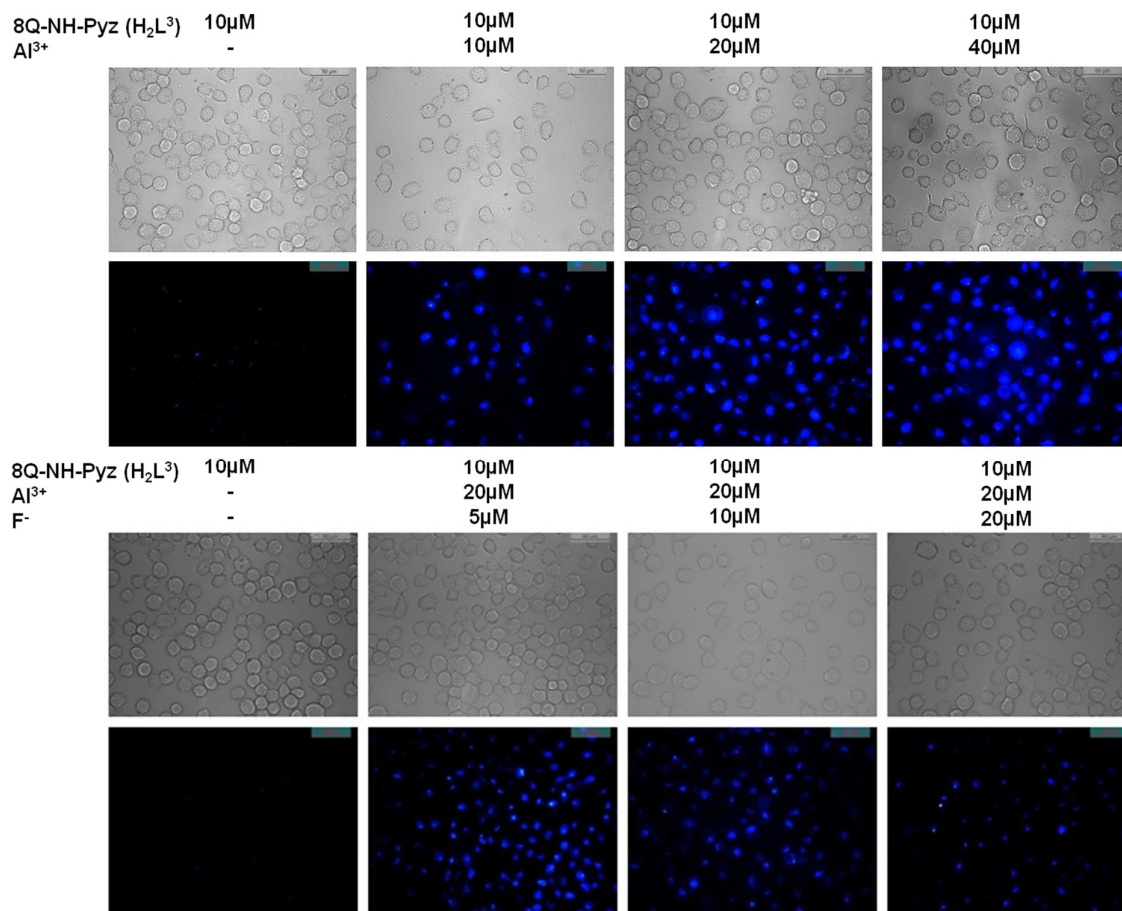


Fig. 12. The phase contrast and fluorescence images of HepG2 cells were captured after incubation with **8Q-NH-Pyz**, (**8Q-NH-Pyz** + Al^{3+}) and (**8Q-NH-Pyz** + Al^{3+} + F^-) for 30 min at 37°C.

Cell imaging studies

Taking into consideration the excellent sensing performance of **8Q-NH-Pyz** towards Al^{3+} , we decided to utilize **8Q-NH-Pyz** for the fluorescence imaging of Al^{3+} into the living HepG2 cell. For this purpose we have determined the cytotoxic effect of **8Q-NH-Pyz** on HepG2 cells, which was found not to affect the cell viability as confirmed by MTT assay (**Fig. S13**). More than 80% cell viability was observed for **8Q-NH-Pyz** at 10 μM after which the viability of HepG2 cells decreases slightly (viability curve). Hence further experiments were carried out with 10 μM of **8Q-NH-Pyz**.

The intracellular imaging behaviours of **8Q-NH-Pyz** on HepG2 cells with the aid of fluorescence microscopy displayed no visible intracellular fluorescence when treated with 10 μM **8Q-NH-Pyz** (**Fig. 12**). Fluorescence images of HepG2 cells were taken separately for another three sets of experiments where cells were incubated with 10 μM **8Q-NH-Pyz** and 10, 20 and 40 μM Al^{3+} for 30 min where bright fluorescence was observed. Similarly, in another sets of experiments, cells were incubated

with 10 μM **8Q-NH-Pyz** + 20 μM Al^{3+} for 30 min followed by addition of 5, 10 and 20 μM F^- for another 30 min and fluorescence images were taken. In this case, HepG2 cells showed almost complete quenching of fluorescence in presence of 20 μM F^- due to removal of Al^{3+} from the **8Q-NH-Pyz**- Al^{3+} complex by F^- ions which manifests a reversible binding of **8Q-NH-Pyz** towards Al^{3+} , satisfying one of the crucial requirements for *in vivo* monitoring of a chemical species.

Moreover, we find out logic gate operation; namely INHIBIT logic gate which involves a particular combination of logic functions AND and NOT. For our system we correlate it by taking two input signals namely Input A (Al^{3+}) and input B (F^-) along with fluorescence signal of the ligand **8Q-NH-Pyz** at 470 nm as output. For input, the presence and absence of Al^{3+} and F^- are assigned as 1 (on-state) and 0 (off-state) respectively. For output, we assign the enhanced fluorescence of **8Q-NH-Pyz** (H_2L^3) as 1 (on-state) and the quenched fluorescence as 0 (off-state) (**Fig. 13 b**, truth table). In the absence of both inputs (Al^{3+} or F^-) **8Q-NH-Pyz** remains in off-state form. Now, input A leads to significant fluorescence enhancement with interaction with free receptor in its occupied state leading to on-state.

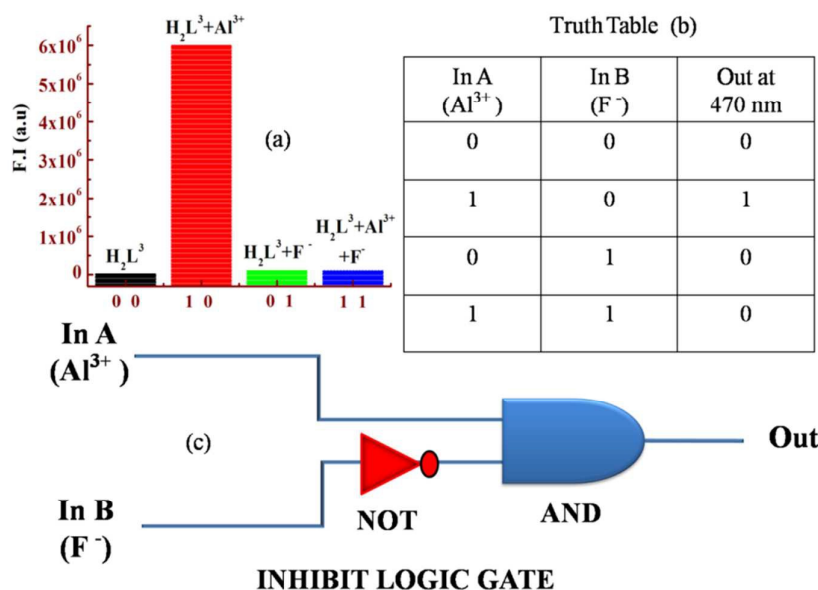


Fig. 13 (a) Output signals (at 470 nm) of the logic gate in presence of different inputs; (b) corresponding truth table of the logic gate; (c) general representation of the symbol of an INHIBIT gate.

Conclusion

In summary, we have synthesized a potential hexa-coordinating (N_3O_3) probe **8Q-NH-Pyz** for selective recognition of Al^{3+} , in presence of large number of background metal ions in purely aqueous medium at pH 7.2 (HEPES buffer), which was found to undergo 1:1 complexation. The probe itself is very weakly fluorescent due to combined PET effect arising out of the transfer of proton from phenolic-OH to azomethine-N in the excited state and rotational isomerisation across the C=N double bond of the azomethine group. It becomes fluorescent only in presence of Al^{3+} which causes PET as well as *cis-trans* isomerisation blocking through selective coordination to the Al^{3+} . The complexation of **8Q-NH-Pyz** to Al^{3+} was confirmed by 1H NMR and ESI-MS⁺ studies and further strengthened by DFT calculations on both the free ligand and its Al^{3+} complex. The Fluorescence titration helps us to delineate $K_d = 1.76 \times 10^{-5}$ M. The reversible binding of Al^{3+} to **8Q-NH-Pyz** was confirmed by reacting with excess F^- both in extra- and intracellular conditions.

Experimental

Materials and Methods.

The 8-Hydroxyquinoline, ethyl chloroacetate (Sigma Aldrich), hydrazine hydrate (Sigma Aldrich), absolute ethanol and salts of Al^{3+} , Ca^{2+} , Cd^{2+} , Co^{2+} , Cr^{3+} , Cu^{2+} , Fe^{3+} , K^+ , Mg^{2+} , Mn^{2+} , Na^+ , Ni^{2+} , Pb^{2+} , Zn^{2+} , Sm^{3+} , Dy^{3+} and La^{3+} were obtained from commercial suppliers and used without further purification. Solvents like MeOH, MeCN etc (Merck, India) were of reagent grade.

Physical Measurements

The Fourier Transform Infrared Spectra ($4000 - 400\text{ cm}^{-1}$) of the ligands were recorded on a Perkin-Elmer RX I FT-IR spectrophotometer with solid KBr disc. Electronic spectra were recorded on an Agilent 8453 Diode-array UV-vis spectrophotometer using HPLC grade H_2O as solvent with 1 cm quartz cuvette in the range 200-900 nm. Fluorescence studies were performed in PTI (Model QM-40) spectrofluorimeter, 1H NMR spectrum were recorded on a Bruker 300 MHz spectrometer using trimethylsilane as an internal standard in DMSO (d_6) and D_2O . ESI-MS⁺ (m/z) of the amine, ligand (**8Q-NH-Pyz** (H_2L^3)) and complex $[Al(L^3)(H_2O)]^+$ were recorded on a HRMS spectrometer (Model: QTOF Micro YA263).

Solution preparation for UV-Vis absorption and fluorescence studies

For both UV-Vis and fluorescence titrations, stock solution of 1.0×10^{-3} M of the probe **8Q-NH-Pyz** was prepared in CH_3CN -MeOH. Similarly, another 1.0×10^{-3} M stock solution of $Al(NO_3)_3 \cdot 9H_2O$ and 1.0×10^{-3} M stock solution of tetrabutyl ammonium fluoride (TBAF) in water were prepared. Other metal ions as well as anions were prepared in MeOH- H_2O . A solution of 10.0 mM HEPES buffer was prepared and pH was adjusted to 7.20 by using HCl and NaOH. Ionic strength of the buffer was maintained at 50 mM (NaCl) throughout the measurements. 2.5 ml of this buffered solution was pipetted out into a cuvette to which was added 20 μM of the probe and metal ions were added incrementally starting from 0 to 36 μM in a regular interval of volume and UV-Vis and fluorescence spectra were recorded for each solution.

Syntheses

Preparation of (Quinolin-8-yloxy)-acetic acid hydrazide (**L**¹).

(a) (Quinolin-8-yloxy)-acetic acid hydrazide was synthesised by the reported method with slight modification.²⁷ In a typical procedure, a mixture of 8-hydroxyquinoline (0.05 mole), ethyl chloroacetate (0.05 mole) and anhydrous K₂CO₃ (0.05 mole) in dry acetone was refluxed on a water bath for 18 h. The mixture was then filtered and solvent was removed under reduced pressure. The resulting solid was purified by column chromatography on silica gel, using petroleum ether: ethyl acetate (3:1) as the eluant to afford **2** (85% yield) as yellow oil.

The resulting (Quinolin-8-yloxy)-acetic acid ethyl ester (0.05 mole) and hydrazine hydrate (0.10 mole) in ethanol were refluxed on a water bath for 5 h. After cooling, the solid that separated out was filtered and washed with water, dried and recrystallized from ethanol. Needle shaped crystals were obtained. Yield 75 % (**L**¹): ¹H NMR (300 MHz DMSO): 4.41(s, 2H, -NH₂), 4.75 (s, 2H, -CH₂), 7.25 (d, 1H), 7.50 - 7.61(m, 3H, -ArH), 8.38 (d, 1H, -ArH), 8.92 (d, 1H, -ArH), 9.46 (s, 1H, -NH) (**Fig. S1**).

Preparation of (3-(3,5-Dimethyl-pyrazol-1-ylmethyl)-2-hydroxy-5-methyl-benzaldehyde. (**HL**²))

2-Chloromethyl-6-carbaldehyde-4-methylphenol (1.515 g, 8.2 mmol) was dissolved in 15 ml dry THF in a round bottom flask. 3,5-Dimethylpyrazole (0.788 g, 8.2 mmol) and triethylamine (Et₃N) (1.659 g, 16.4 mmol) were dissolved in 10 ml dry THF and this mixture was added dropwise to the 2-chloromethyl-6-carbaldehyde-4-methylphenol solution. A rapid precipitation of Et₃N•HCl was observed and the colour of the solution turned to bright yellow (Scheme 1). After 24 hours of stirring, the precipitate was filtered off and subsequently the solvent (THF) was removed under reduced pressure to afford an oily product that yielded a yellow crystalline solid after 2 days at 4 °C. The solid product was then filtered and washed with cold ether. Yield 72%. ¹H NMR (in DMSO-d₆): δ in ppm 2.23–2.28 (9 H, m, -ArCH₃), 5.27 (2H, s, -CH₂), 7.09 (1H, s, -ArH), 7.27 (1H, s, -ArH), 7.28 (1H, s, -ArH), 9.88 (1H, s, -CHO), 11.23 (1H, brs, -ArOH) (**Fig. S2**).

Preparation of (Quinolin-8-yloxy)-acetic acid [3-(3,5-dimethyl-pyrazol-1-ylmethyl)-2-hydroxy-5-methyl-benzylidene]-hydrazide. **8Q-NH-Pyz** (**H₂L³**)

L¹ (0.434 g, 2 mmol) was dissolved in 25 mL MeOH. To this solution was added **HL**² (0.488 g, 2 mmol) drop wise and refluxed for 2h and then the reaction mixture was filtered out and evaporated to dryness in rota-evaporator. White solid of **H₂L³** obtained was purified by recrystallization from ethanol. (yield, 78.34%). : ¹H-NMR (in DMSO-d₆) (δ, ppm): 2.08-2.16(s,9H₃), 4.95(s,2H,-CH₂), 5.09(s,2H,-CH₂),5.83 (s,1H), 6.62 (s, 1H, -ArH), 7.20 (s,1H,-ArH), 7.30 (d,1H,-ArH), 7.50 - 7.62 (m,3H, -ArH), 8.38 (d,1H,-ArH), 8.46 (s, 1H, azomethine), 8.96 (d,1H,-ArH), 11.74 (s,1H,-OH) and 12.35 (s,1H,-NH).(**Fig. S3**). ESI-MS+ (m/z): 444.20 (**8Q-NH-Pyz** (**H₂L³**)+H⁺) (**Fig. S5**).

Computational details

Ground state electronic structure calculations in methanol solution of both the ligand and complex have been carried out using DFT method²⁸ associated with the conductor-like polarizable continuum model (CPCM).²⁹ Becke's hybrid function³⁰ with the Lee-Yang-Parr (LYP) correlation function³¹ were used throughout the study. The geometry of the ligand and complex were fully optimized without any symmetry constraints. The nature of all stationary points for both the free ligand and its Al³⁺ complex were confirmed by carrying out normal mode analysis. On the basis of the optimized ground state geometry, the absorption spectral properties **8Q-NH-Pyz** and complex [Al(**L**³)(H₂O)]⁺ in water were calculated by time-dependent density functional theory (TDDFT)³² associated with the conductor-like polarizable continuum model (CPCM).²⁹ We have computed the lowest 40 singlet–singlet transitions and the presence of electronic correlation in the TDDFT (B3LYP) method³³ enables to get accurate electronic excitation energies. For H atoms we used 6-31G basis set; for C, N, O and Al atoms we employed 6-31+G(d) basis sets for the optimization of the ground state. The calculated electron density plots for frontier molecular orbitals were prepared by using Gauss View 5.1 software. All the calculations were performed with the Gaussian 09W software package.³⁴ Gauss Sum 2.1 program³⁵ was used to calculate the molecular orbital contributions from groups or atoms.

Cell culture

Human hepatocellular liver carcinoma cells, HepG2 cell lines, were procured from National Center for Cell Science, Pune, India, and used throughout the study. Cells were cultured in DMEM (Gibco BRL) supplemented with 10% FBS (Gibco BRL), and a 1% antibiotic mixture containing Penicillin, Streptomycin and Gentamicin (Gibco BRL) at 37°C in a humidified incubator with 5% CO₂ and cells were grown to 60-80% confluence, harvested with 0.025% trypsin (Gibco BRL) and 0.52 mM H₂EDTA²⁻ (Gibco BRL) in phosphate-buffered saline (PBS), plated at the desired cell concentration and allowed to re-equilibrate for 24 h before any treatment.

Cell Cytotoxicity Assay

To test the cytotoxicity of **8Q-NH-Pyz** assay was performed as per the procedure described earlier.³⁶ After treatment with **8Q-NH-Pyz** at different doses of 1, 10, 20, 40, 60, 80 and 100 μM, respectively, for 12 h, 10 μl of MTT solution (10 mg/ml PBS) was added to each well of a 96-well culture plate and again incubated continuously at 37°C for a period of 3 h. All the media were removed from wells and 100 μl acidic isopropyl alcohol was added into each well. The intracellular formazan crystals (blue-violet) formed were solubilized with 0.04 N acidic isopropyl alcohol and absorbance of the solution was measured at 595 nm with a microplate reader (Model: THERMO MULTI SCAN EX). The cell viability was expressed as the optical density ratio of the treatment to control. Values were expressed as mean ± standard errors of three

independent experiments. The cell cytotoxicity was calculated as % cell cytotoxicity = 100% - % cell viability (Fig. S12).

Cell Imaging Study

HepG2 Cells were incubated with 10 μM 8Q-NH-Pyz (the stock solution 1 mM was prepared by dissolving 8Q-NH-Pyz to the mixed solvent (DMSO: water = 1:9 (v/v)) in the culture medium, allowed to incubate for 30 min at 37 $^{\circ}\text{C}$. After incubation, cells were washed twice with phosphate-buffered saline (PBS). Bright field and fluorescence images of HepG2 cells were taken by a fluorescence microscope (Leica DM3000, Germany) with an objective lens of 40X magnification. Fluorescence images of HepG2 cells were taken separately from another set of experiment where cells incubated separately with 10 μM 8Q-NH-Pyz and 10, 20 and 40 μM Al^{3+} for 30 min. Similarly, in another set of experiment, cells were incubated with 10 μM 8Q-NH-Pyz + 20 μM Al^{3+} in three sets and then 5, 10 and 20 μM of F^{-} were added separately for 30 min and fluorescence images were taken. HepG2 cells showed almost complete quenching of fluorescence due to removal of Al^{3+} from the complex.

Acknowledgement

Financial support from DST (Ref. SR/S1/IC-20/2012) New Delhi is gratefully acknowledged.

References

- (a) G. Sivaraman, T. Anand and D. Chellappa, *Analyst*, 2012, **137**, 5881; (b) K. Tayade, S. K. Sahoo, B. Bondhopadhyay, V. K. Bhardwaj, N. Singh, A. Basu, R. Bendre, A. Kuwar, *Biosensors and Bioelectronics*, 2014, **61**, 429; (c) G. Sivaraman and D. Chellappa, *J. Mater. Chem. B.*, 2013, **1**, 5768; (d) G. Sivaraman, V. Sathiyaraja and D. Chellappa, *J. of Luminescence*, 2014, **145**, 480; (e) T. Anand, G. Sivaraman and D. Chellappa, *J. Photochem. Photobiol. A: Chem.*, 2014, **281**, 47. (f) C. Arivazhagan, R. Borthakur and S. Ghosh, *Organometallics*, 2015, **34**, 1147–1155; (g) O. Sunnapu, N. G. Kotla, B. Maddiboyina, S. Singaravadiel and G. Sivaraman, *RSC Adv.*, 2016, **6**, 656; (h) K. M. Vengaian, C. D. Britto, K. Sekar, G. Sivaraman and S. Singaravadiel, *RSC Adv.*, 2016, **6**, 7668; (i) G. Sivaraman, T. Anand and D. Chellappa, *RSC Adv.*, 2012, **2**, 10605; (j) G. Sivaraman, T. Anand and D. Chellappa, *RSC Adv.*, 2013, **3**, 17029; (k) T. Anand, G. Sivaraman, P. Anandh, D. Chellappa and S. Govindarajan, *Tet. Lett.*, 2014, **55**, 671; (l) G. Sivaraman, T. Anand and D. Chellappa, *Anal. Methods*, 2014, **6**, 2343; (m) G. Sivaraman, T. Anand, and D. Chellappa, *ChemPlusChem* 2014, **79**, 1761.
- K. Soroka, R. S. Vithanage, D. A. Phillips, B. Walker and P. K. Dasgupta, *Anal. Chem.* 1987, **59**, 629.
- J. R. Lakowicz, *Topics in Fluorescence Spectroscopy: Probe Design and Chemical Sensing*, Kluwer Academic Publishers, New York, 2002, 4.
- M. G. Soni, S. M. White, W. G. Flamm and G. A. Burdock, *Regul. Toxicol. Pharmacol.* 2001, **33**, 66.
- (a) T. P. Flaten and M. Odegard, *Food Chem. Toxicol.* 1988, **26**, 959; (b) J. Ren and H. Tian, *Sensors*, 2007, **7**, 3166; (c) R. A. Yokel, *Neurotoxicology*, 2000, **21**, 813.
- (a) O. Y. Nadzhafova, S.V. Lagodzinskaya, V. V. Sukhan, *J. Anal. Chem.* 2001, **561**, 78; (b) M.J. Ahmed, J. Hossan, *Talanta*. 1995, **42**, 1135; (c) M. Ahmad, R. Narayanaswamy, *Sensors Actuators B Chem.* 2002, **81**, 259.
- R. Flarend and D. Elmore, Aluminum-26 as a biological tracer using accelerator mass spectrometry, in: P. Zatta, A.C. Alfrey (Eds.), *Aluminum in Infant's Health and Nutrition*, 5 World Scientific, Singapore, 1997, 16.
- J. L. McDonald-Stephens and G. Taylor, *Plant Physiol.*, 1995, **145**, 327.
- R. F. Fleming and R.M. Lindstrom, *J. Radioanal. Nucl. Chem.* 1987, **113**, 35.
- J.C. Rouchaud, N. Boisseau and M. Fedoroff, *J. Radioanal. Nucl. Chem. Lett.* 1993, **175**, 25.
- B. Rietz, K. Heydorn and G. Pritzl, *J. Radioanal. Nucl. Chem.* 1997, **216**, 113.
- M. A. Lovell, *Ann. Neurol.* 1993, **33**, 36.
- S. Knežević, R. Milačić and M. Veber, *J. Anal. Chem.*, 1998, **362**, 162.
- (a) J. W. Zhu, Y. Qin and Y. H Zhang, *Anal. Chem.*, 2010, **82**, 436; (b) T. Y. Han, X. Feng, B. Tong, J. B. Shi, L. Chen, J. G. Zhi and Y. P. Dong, *Chem. Commun.*, 2012, **48**, 416; (c) S. Anbu, S. Shanmugaraju, R. Ravishankaran, A. A. Karande and P. S. Mukherjee, *Dalton Trans.* 2012, **41**, 13330.
- (a) U. E. Spichiger-Keller, *Chemical Sensors and Biosensors for Medical and Biological Applications*, Wiley-VCH, Weinheim, Germany, 1998; (b) V. Amendola, L. Fabbri, F. Forti, M. Licchelli, C. Mangano, P. Pallavicini, A. Poggi, D. Sacchi and A. Taglietti, *Coord. Chem. Rev.* 2006, **250**, 273; (c) K. Rurack and U. Resch-Genger, *Chem. Soc. Rev.*, 2002, **31**, 116; (d) P. T. Srinivasan, T. Viraraghavan and K. S. Subramanian, *Water SA*, 1999, **25**, 47.
- (a) T. Mistri, R. Alam, R. Bhowmick, S. K. Mandal, M. Dolai, A. R. Khudabukhsh, M. Ali, *Analyst*, DOI: 10.1039/C3AN02255B; (b) M. Arduini, P. Tecilla, *Chem. Commun.*, 2003, **25**, 1606; (c) J. S. Kim, J. Vicens, *Chem. Commun.*, 2009, **45**, 4791; (d) S. Kim, J. Y. Noh, K. Y. Kim, J. H. Kim, H. K. Kang, S. W. Nam, S. H. Kim, S. Park, C. Kim, J. Kim, *Inorg. Chem.*, 2012, **51**, 3597; (e) F. K. Hau, X. M. He, W. H. Lam, V. W. Yam, *Chem. Commun.*, 2011, **47**, 8778; (f) Y. Lu, S. S. Huang, Y. Y. Liu, S. He, L. C. Zhao, X. S. Zeng, *Org. Lett.*, 2011, **13**, 5274; (g) D. Maity, T. Govindaraju, *Chem. Commun.*, 2010, 46, 4499; (h) Y. Dong, J. F. Li, X. X. Jiang, F. Y. Song, Y. X. Cheng, C. J. Zhu, *Org. Lett.*, 2011, **13**, 2252; (i) L. Wang, W. Qin, X. Tang, W. Dou, W. Liu, Q. Teng, and X. Yao, *Org. Biomol. Chem.*, 2010, **8**, 3751; (j) K. K. Upadhyay and A. Kumar, *Org. Biomol. Chem.*, 2010, **8**, 4892; (k) A. Sahana, A. Banerjee, S. Das, S. Lohar, D. Karak, B. Sarkar, S. K. Mukhopadhyay A. K. Mukherjee and D. Das, *Org. Biomol. Chem.*, 2011, **9**, 5523.
- (a) W-H Ding, W. Cao, X-J. Zheng, D-C. Fang, W-T Wong, and L-P Jin; *Inorg. Chem.*, 2013, **52**, 7320 (b) D. Maity and T. Govindaraju, *Inorg. Chem.*, 2010, **49**, 7229; (c) D. Maity

- and T. Govindaraju, *Chem. Commun.* 2010, **46**, 4499; (d) S. Sinha, R. R. Koner, S. Kumar, J. Mathew, Monisha, P. V., I. Kazia and S. Ghosh, *RSC Adv.* 2013, **3**, 345.
- 18 (a) S. Kim, J. Y. Noh, K. Y. Kim, J. H. Kim, H. K. Kang, S-W. Nam, S. H. Kim, S. Park, C. Kim and J. Kim; *Inorg.Chem.*, 2012, **51**, 3597; (b) C-H. Chen, D-J. Liao, C.-F. Wan and A-T. Wu; *Analyst*, 2013, **138**, 2527.
- 19 S. H. Kim, H. S. Choi, J. Kim, S. J. Lee, D. T. Quang and J. S. Kim, *Org. Lett.*, 2010, **12**, 560.
- 20 M. Dong, Y.M. Dong, T.H. Ma, Y.W. Wang and Y. Peng, *Inorg. Chim. Acta.*, 2012, **381**, 137.
- 21 T. Han, X. Feng, B. Tong, J. Shi, L. Chen, J. Zhic and Y. Dong, *Chem. Commun.*, 2012, **48**, 416.
- 22 X. Sun, Y. W. Wang and Y. Peng, *Org. Lett.*, 2012, **14**, 3420.
- 23 K. K. Upadhyay and A. Kumar, *Org. Biomol. Chem.*, 2010, **8**, 4892.
- 24 J. Y. Jung, S. J. Han, J. Chun, C. Lee and J. Yoon, *Dyes Pigm.*, 2012, **94**, 423.
- 25 T. Anand, G. Sivaraman, A. Mahesh and D. Chellappa, *Anal. Chim. Acta.*, 2015, 853, 596.
- 26 (a) K. M. Vengaian, C. D. Britto, G. Sivaraman, K. Sekar and S. Singaravadiivel, *RSC Adv.*, 2015, **5**, 94903; (b) T. Anand, G. Sivaramana, M. Iniya, A. Siva and D. Chellappa, *Anal. Chim. Acta*, 2015, **876**, 1; (c) G. Sivaraman and D. Chellappa, *J. Mater. Chem. B.*, 2013, **1**, 5768.
- 27 M. Ahmed, R. Sharma, D. P. Nagda, J. L. Jatand G. L. Talesara, *Arkivoc*, 2006, xi, 66.
- 28 R. G. Parr, W. Yang, *Density Functional Theory of Atoms and Molecules*, Oxford University Press, Oxford, 1989.
- 29 (a) V. Barone and M. Cossi, *J. Phys. Chem. A.*, 1998, **102**, 1995; (b) M. Cossi and V. Barone, *J. Chem. Phys.*, 2001, **115**, 4708; (c) M. Cossi, N. Rega, G. Scalmani and V. Barone, *J. Comp. Chem.*, 2003, **24**, 669.
- 30 A. D. Becke, *J. Chem. Phys.*, 1993, **98**, 5648.
- 31 C. Lee, W. Yang and R. G. Parr, *Phys. Rev.*, 1998, **37**, 785.
- 32 (a) M. E. Casida, C. Jamoroski, K. C. Casida and D. R. Salahub, *J. Chem. Phys.*, 1998, **108**, 4439; (b) R. E. Stratmann, G. E. Scuseria and M. J. Frisch, *J. Chem. Phys.*, 1998, **109**, 8218; (c) R. Bauernschmitt and R. Ahlrichs, *Chem. Phys. Lett.*, 1996, **256**, 454.
- 33 (a) T. Liu, H. X. Zhang and B. H. Xia, *J. Phys. Chem. A.*, 2007, **111**, 8724; (b) X. Zhou, H. X. Zhang, Q. J. Pan, B. H. Xia and A. C. Tang, *J. Phys. Chem. A.*, 2005, **109**, 8809; (c) X. Zhou, A. M. Ren and J. K. Feng, *J. Organomet. Chem.*, 2005, **690**, 338. (d) A. Albertino, C. Garino, S. Ghiani, R. Gobetto, C. Nervi, L. Salassa, E. Rosenverg, A. Sharmin, G. Viscardi, R. Buscaino, G. Cross and M. Milanese, *J. Organomet. Chem.*, 2007, **692**, 1377.
- 34 M. J. Frisch, G. W. Trucks, H. B. Schlegel, G. E. Scuseria, M. A. Robb, J. R. Cheeseman, G. Scalmani, V. Barone, B. Mennucci, G. A. Petersson, H. Nakatsuji, M. Caricato, X. Li, H. P. Hratchian, A. F. Izmaylov, J. Bloino, G. Zheng, J. L. Sonnenberg, M. Hada, M. Ehara, K. Toyota, R. Fukuda, J. Hasegawa, M. Ishida, T. Nakajima, Y. Honda, O. Kitao, H. Nakai, T. Vreven, J. A. Montgomery Jr., J. E. Peralta, F. Ogliaro, M. Bearpark, J. J. Heyd, E. Brothers, K. N. Kudin, V. N. Staroverov, R. Kobayashi, J. Normand, K. Raghavachari, A. Rendell, J. C. Burant, S. S. Iyengar, J. Tomasi, M. Cossi, N. Rega, J. M. Millam, M. Klene, J. E. Knox, J. B. Cross, V. Bakken, C. Adamo, J. Jaramillo, R. Gomperts, R. E. Stratmann, O. Yazyev, A. J. Austin, R. Cammi, C. Pomelli, J. W. Ochterski, R. L. Martin, K. Morokuma, V. G. Zakrzewski, G. A. Voth, P. Salvador, J. J. Dannenberg, S. Dapprich, A. D. Daniels, Ö. Farkas, J. B. Foresman, J. V. Ortiz, J. Cioslowski, D. J. Fox, Gaussian 09, (Revision A.1), Gaussian, Inc., Wallingford, CT 2009.
- 35 N. M. O'Boyle, A. L. Tenderholt and K. M. Langner, *J. Comp. Chem.*, 2008, **29**, 839.
- 36 R. Alam, T. Mistri, A. Katarkar, K. Chaudhuri, S. K. Mandal, A. R. Khuda-Bukhsh, K. K. Das and M. Ali, *Analyst*, 2014, **139**, 4022.

A novel 8-hydroxyquinoline—pyrazole based highly sensitive and selective Al(III) sensor in purely aqueous medium with intracellular application: experimental and computational studies.

Abu Saleh Musha Islam^a, Rahul Bhowmick^a, Hasan Mohammad^a, Atul Katarkar^b, Keya Chaudhuri^b and Mahammad Ali*^a

A new 8-hydroxyquinolin-pyrazole based probe senses Al³⁺ and hence Al³⁺—8Q-NH-Pyz complex mediated F⁻ in purely aqueous medium.

